Non-Invasive Visualization of Melanin and Melanocytes by Reflectance-Mode Confocal Microscopy

Toyonobu Yamashita,* Tomohiro Kuwahara,* Salvador González,† and Motoji Takahashi*
*Shiseido Research Center (Shin-Yokohama), Yokohama, Japan; †Wellman Laboratories of Photomedicine, Department of Dermatology, Massachusetts General Hospital, Harvard Medical School, Boston, Massachusetts, USA

In vivo **visualization of epidermal melanin was performed by reflectance-mode confocal microscopy (RCM). Firstly, we examined the distribution of epidermal melanin in pigmented animals and compared with that of the human skin. Melanocytes in the skin of pigmented animals were found to accumulate a large amount of melanin that can be easily visualized because of its brightness. Their RCM images correlated well with the Fontana–Masson-stained sections for melanin. In contrast, in the human skin, typical dendritic melanocytes were hardly observed even in pigmented lesions, although supranuclear melanin caps were easily visible. These results suggested that human melanocytes rapidly transfer the produced melanin to keratinocytes and do not accumulate it. Secondly, to elucidate the production of melanin by human melanocytes, we evaluated the changes of melanin after a single ultraviolet (UV) exposure. The melanin-accumulating melanocytes were clearly visualized during the skin pigmentation process. The RCM images showed the brightness because of melanin gradually increased from day 4, then dendrite-elongated melanocytes appearing from day 8, and finally melanin caps formed from day 29. In conclusion, RCM successfully evidenced the difference in melanin distribution between the pigmented animals and humans, and the UV-induced pigmentation process *in vivo* as well.**

Keywords: melanin/melanocyte/non-invasive method/reflectance-mode confocal microscopy/UVB
J Invest Dermatol 124:235–240, 2005

Pigmentation of the skin is related to the amount of melanin that provides protection against ultraviolet (UV) radiation. Melanins are synthesized in tyrosinase-containing melanosomes within the melanocyte. The melanosomes are transferred to keratinocytes through the tips of dendrites of the melanocyte (Mottaz and Zelickson, 1967; Klaus, 1969; Jimbow *et al*, 1976; Marks and Seabra, 2001). The examination of tissue specimens has revealed that the highest density of melanin, forming melanosome clusters is present in the epidermal basal layer (Gates and Zimmermann, 1953; Szabo, 1969; Montagna and Carlisle, 1991; Byers *et al*, 2003). Factors that regulate the pattern of melanosome accumulation exist within keratinocytes (Minwalla *et al*, 2001). Recently, the retrograde microtubular motor cytoplasmic dynein was suggested to mediate the aggregation of melanosomes (Byers *et al*, 2003). In humans, aggregated melanosomes are located above the nucleus of the epidermal basal cells, presenting themselves as "supranuclear melanin caps" (Gates and Zimmermann, 1953) for protecting the nucleus from UV-induced DNA damage (Kobayashi *et al*, 1998). In pigmented animals, however, the existence of supranuclear melanin caps has not been clear.

For understanding the metabolism of melanin, it is important to know its distribution in each epidermal layer. In particular, knowing the amount of melanin and its detailed distribution in the basal layer where the melanocytes exist is critical for evaluating their activity. Reflectance-mode confocal microscopy (RCM) allows non-invasive optical sectioning of each layer of the skin in real time (Corcuff *et al*, 1993; Rajadhyaksha *et al*, 1995, 1999; Huzaira *et al*, 2001; Swindle, 2003), with melanin as the main endogenous contrast (Rajadhyaksha *et al*, 1995), and enables one to image the epidermis at a cellular level.

Since the behavior of melanocytes in response to UV irradiation has been examined previously using biopsy specimens (Mizuno, 1968; Jimbow and Uesugi, 1982), it has been hard to obtain the time course of changes for the human skin in detail.

Here, we aimed to test the applicability of RCM for non-invasive visualization of melanin *in vivo*. Firstly, we assessed the distribution of melanin in the epidermal basal layer of the human skin and that of pigmented animals' skin. Secondly, the changes of melanin in the UV-exposed human skin were examined.

Results

Different melanin distribution in the epidermal basal layers of the human and the pigmented animals' skin RCM images of normal human skin (forearm and age-dependent pigmentary lesions on the face) were compared with those of the back skin of pigmented animals. As

Abbreviations: DOPA, 3,4-dihydroxyphenylalanine; MED, minimal erythema dose; RCM, reflectance-mode confocal microscope; UV, ultraviolet

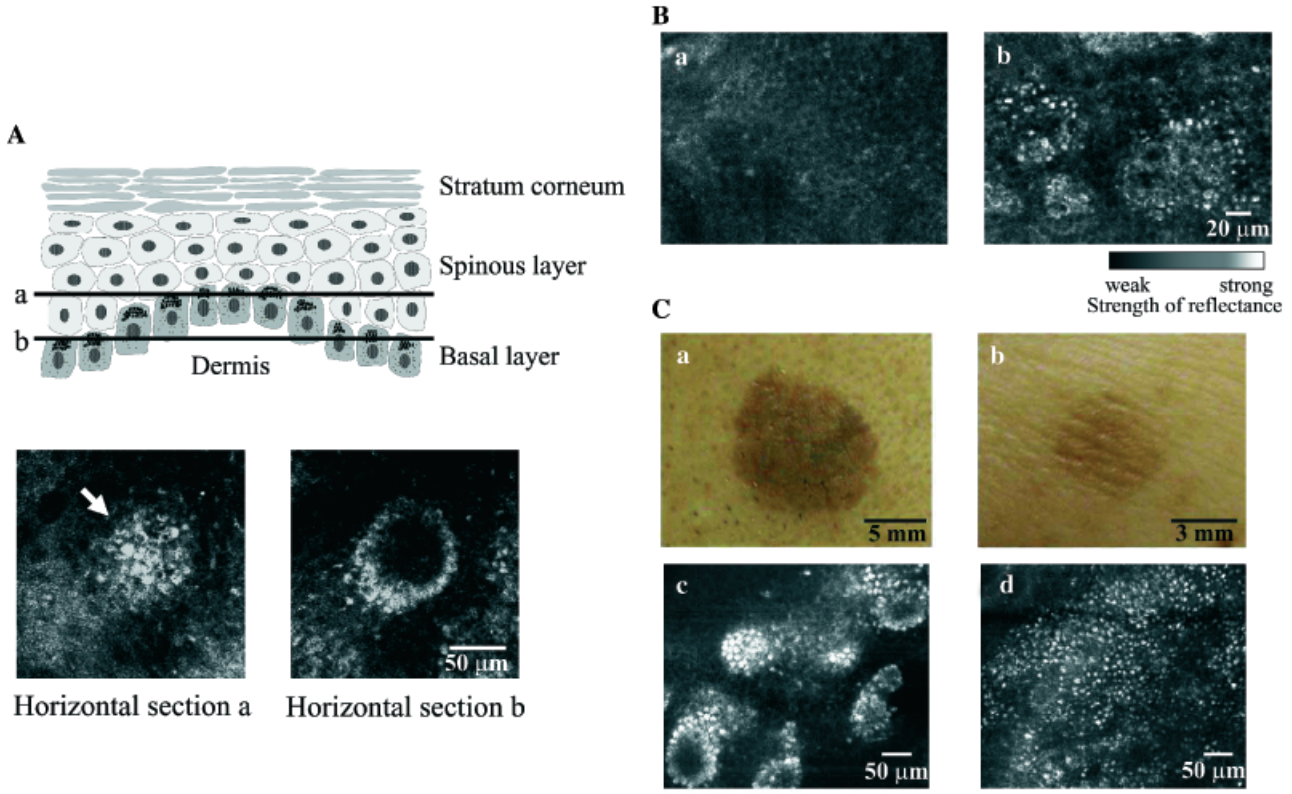

Figure 1
Reflectance-mode confocal microscopy (RCM) visualization of melanin in the human skin. (*A*) RCM images of the forearm at the dorsal side were taken at planes a and b shown in the scheme of the vertical section of epidermis. The back-scattered light from the supranuclear melanin caps (*arrows*) is strong. (*B*) RCM images of the forearm show less back-scattered light from the basal layer at the volar side (*a*) than at the dorsal side (*b*). The light scattering is attributed to melanin. (*C*) Photographs by a digital camera (*a* and *b*) and RCM images (*c* and *d*) of an age-dependent pigmentary lesion on the face are shown. The RCM images (*c* and *d*) clearly show supranuclear melanin caps (*bright regions*), but recognition of melanocytes is difficult.

expected, the greater the degree of skin pigmentation, the greater was the reflectance signal from the epidermal layers in humans. A strong reflectance derived from melanin was observed especially in the epidermal basal layer. The brightness of the basal layer was clearly stronger on the dorsal than on the volar forearm (Fig 1*B*, *b vs a*). The presence of vesicle-like structures representing the supranuclear melanin caps was observed (Fig 1*A*). Melanocytes were, however, hardly observed in the normal skin. In the age-dependent pigmentary lesions (Fig 1*C*, *a* and *b*), melanocytes were also hardly recognized although

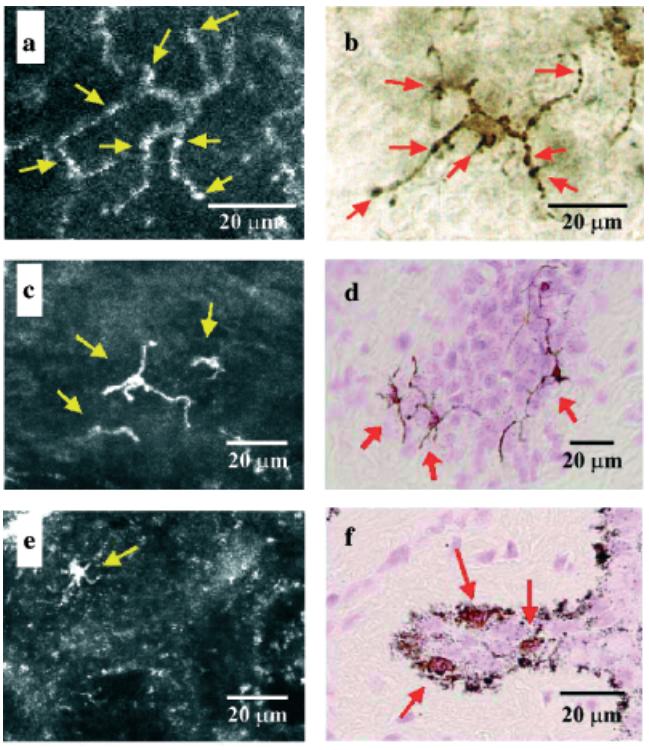

Figure 2
Reflectance-mode confocal microscopy (RCM) visualization of melanosomes and melanocytes in pigmented animals' skin. (*a*, *b*) Comparison between the RCM image (*a*) and 3,4-dihydroxyphenylalanine (DOPA) staining (*b*) of the epidermal sheet of a (HR-1 × HR/De) F_1 mouse: the RCM image (*a*) correlates well with the DOPA-stained epidermal sheet (*b*) and both show melanosome-like vesicles (*arrows*). (*c*, *d*) Comparison between the RCM image (*c*) with Fontana–Masson-stained horizontal section (*d*) of the dorsal skin of a Weiser–Maples guinea-pig: melanocytes (*arrows*) with high brightness are clearly observed with RCM (*c*), and histologically confirmed with Fontana–Masson staining (*d*). (*e*, *f*) Comparison between the RCM image (*e*) and Fontana–Masson-stained horizontal section (*f*) of the dorsal skin of a Yucatan micropig: melanocytes (*arrows*) are observed with both the methods (*e* and *f*). The epidermal layers were 31 μm [(HR-1 × HR/De) F_1 mouse], 22 μm (Weiser–Maples guinea-pig), and 69 μm thick (Yucatan micropig), respectively, as measured on hematoxylin–eosin-stained transversal sections.

supranuclear melanin caps were more clearly observed (Fig 1*C*, *c* and *d*).

In contrast, melanocytes were easily observed in the skin of the pigmented animals such as (HR-1 × HR/De) F_1 mice, Weiser–Maples guinea-pigs, and Yucatan micropigs (Fig 2). The image of the melanocytes obtained by 3,4-dihydroxyphenylalanine (DOPA) staining (Fig 2*b*) of the epidermal sheet of (HR-1 × HR/De) F_1 mice morphologically corresponded to that observed non-invasively with RCM (Fig 2*a*). Careful observation revealed spotted DOPA-positive areas (see *arrows* in Fig 2*b*), localized in the dendrites of the melanocytes, which correspond to regions of high brightness in the RCM images (see *arrows* in Fig 2*a*).

The Fontana–Masson staining of the sections of Weiser–Maples guinea-pigs (Fig 2*d*) showed the shape of melanocytes as being very similar to that observed with RCM (Fig 2*c*). In the Yucatan micropig skin, melanocytes could be visualized as in the mouse and the guinea-pig, except that dispersed melanosomes were also found in the epidermal basal layer in the RCM images (Fig 2*e*) and Fontana–Masson stainings (see the small spots in Fig 2*f*). These results indicate that DOPA- (Fig 2*b*) and Fontana–Masson-stained regions (Fig 2*d* and *f*) may correspond to those bright areas seen in the RCM images (Fig 2*a*, *c*, and *e*), and are closely related to the presence of melanin. In pigmented animals, melanocytes showed a strong reflectance compared with the background and thus, were easily visualized. The supranuclear melanin caps were, however, not clearly visible. These results suggest that, in contrast to humans, in the pigmented animals the melanin remains accumulated in the melanocytes, and the supranuclear melanin caps seem to be hardly formed.

Changes in the melanin content and localization in the human epidermal basal layer upon UV exposure The volar forearm skin after a single UV exposure (2.5 minimal erythema dose (MED)) was examined along the time. The highest intensity of erythema occurred 2 d after UV exposure. It decreased gradually thereafter and completely disappeared by day 29. The maximum darkening was observed on day 8 and gradually decreased thereafter, but it does not return to the original state even on day 70 (Fig S1). In the observation of the basal layer, the brightness in the RCM images temporarily decreased after UV exposure (Fig 3, *b vs a*), and gradually increased from day 4. We could observe activated melanocytes with accumulated melanin 8 d after UV exposure (Fig 3*c* and *d*). Thereafter, the melanocytes gradually disappeared and could no longer be observed in the RCM images. Instead, the supranuclear melanin caps became clear from day 29 (Fig 3*e* and *f*).

Discussion

Melanin visualization by RCM The distribution of melanin in the human skin was evaluated non-invasively with RCM. An image with strong contrast was observed in the basal layer (Fig 1*A*), because of the reflectance of the melanin within the melanosomes. A structure of supranuclear melanin caps consisting of accumulated melanosomes immediately above the nucleus of each basal cell was also observed (Fig 1*A*). Generally, when light passes from a layer with low refractivity to one with a high refractivity, a strong reflection occurs at the interface. Melanin has a strong refractivity ($n = 1.7$) compared with the epidermis ($n = 1.34$–1.4), which is considered to be the reason for its strong reflectance and image with a high contrast compared with the surrounding area (Rajadhyaksha *et al*, 1995). Interestingly, the brightness was not homogeneous in the basal layer (Fig 1*Bb*). This suggests that the distribution of melanin is not uniform and is dependent on the presence of the melanocytes. When focused in the vertical direction, the brightness was lower in the spinous layer than in the basal layer (data not shown). A possible explanation for the lower brightness in the spinous layer could be that the aggregated melanosomes suffer dispersion and/or degradation. We observed, however, that the spinous layer above the basal layer region with abundant melanin as supranuclear caps still presents a relatively stronger brightness when compared with the surrounding spinous area. This might be because the melanin in the basal layer moves to the upper spinous layer with the differentiation of the basal keratinocytes, and in consequence, the brightness of the spinous layer becomes stronger. Therefore, the reflectance image obtained by RCM seems to strongly depend on the distribution of melanin.

Comparison of the melanin distribution between human and pigmented animals A clear difference in the melanin distribution was observed between the human skin (Fig 1*A*) and the pigmented animal skin (Fig 2). Although supranuclear melanin caps were clearly evidenced in the normal human skin, melanocytes were not easily identified (Fig 1). This might be because the melanin produced by the melanocytes in the basal layer exists in larger amount in the keratinocytes (to where the melanin is transferred) than in the melanocytes themselves. The contrast of the melanocytes is thus lower than that of the surrounding keratinocytes. Furthermore, since melanocytes could not be confirmed even in the age-dependent pigmentary lesion in humans (Fig 1*C*, *c* and *d*), the melanosomes produced by the melanocytes are likely to be rapidly transferred to keratinocytes. Figure 1*C*, *c* and *d* show many supranuclear melanin caps localized in the entire field, which makes it quite difficult to distinguish the shape of melanocytes, although they should be certainly present in the basal layer. This matter awaits further investigations by accurate immunostaining with specific antibodies directed to melanocyte markers. In humans, except in pathological cases, the melanocyte itself does not accumulate melanosomes but transfers the produced melanosomes immediately to the keratinocytes. Recently, Hara *et al* (2000) reported the participation of kinesin, a molecule that participates in microtubule-associated transport of organelles and is highly expressed in human melanocytes, in the transfer of melanosomes within the dendrites of melanocytes.

On the other hand, in pigmented animals, the melanocytes were relatively easy to observe, but clear supranuclear melanin caps were not visualized (Fig 2). The contrast of the melanocytes is high in the pigmented animals examined in this study. A possible explanation could be that their melanocytes retain a large number of melano-

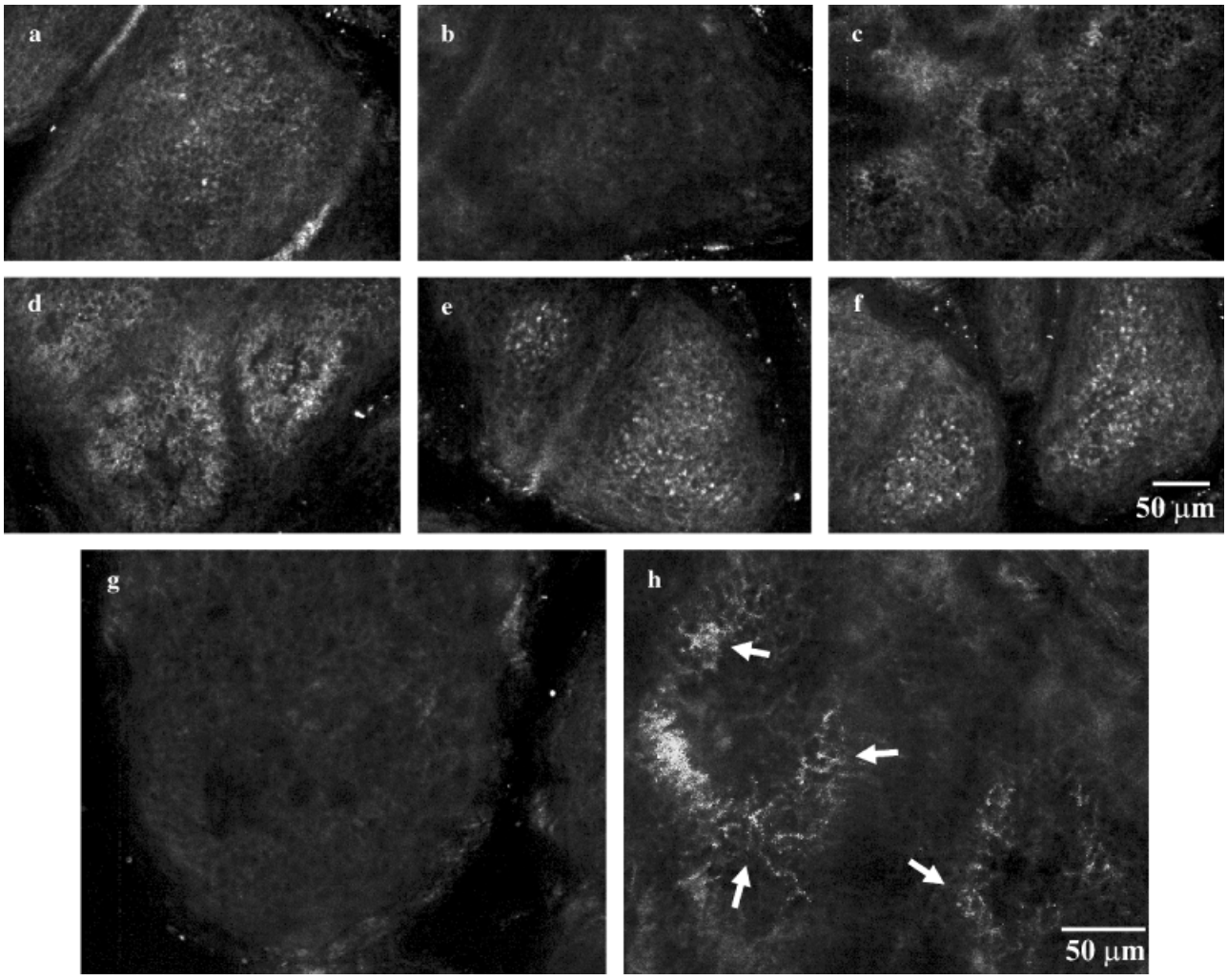

Figure 3
Reflectance-mode confocal microscopy (RCM) visualization of melanocytes in the human volar forearm skin after ultraviolet (UV) exposure. (*a*) The changes after a single exposure UV (2.5 minimal erythema dose) were followed by RCM imaging. Before UV exposure, a slight reflectance depending on the melanin content is observed. (*b*) Three days after UV exposure, the images become dark. (*c*) On day 8, the intensity of reflectance is increased, suggesting that melanin is being produced by melanocytes. (*d*) After 18 d, the reflectance becomes stronger. (*e*, *f*) Twenty-nine and 70 d after UV exposure, the supranuclear melanin caps are clearly observed. (*g*, *h*) Expanded images of day 8 after UV exposure, except that images were taken with enhanced contrast. (*h*) UV-exposed area with clearly visible dendritic melanocytes (*arrows*), and (*g*) an area not exposed to UV, for comparison.

somes because of a slow transfer of melanosomes to the surrounding keratinocytes when compared with the human melanocytes. Also, a low level of melanosome aggregation in keratinocytes may be involved.

Assessment of melanin production after UV exposure In the serial responses of the human volar forearm skin, the brightness of the basal layer in RCM images was decreased on days 2–4 after the UV exposure (Fig 3*b*), when compared with pre-exposure (Fig 3*a*). According to our RCM analysis, a possible explanation for this temporary decrease of brightness may be the following: keratinocytes rich in supranuclear melanin caps proliferate rapidly after UV exposure and move upward bearing a large part of the melanin, thus leaving the epidermal basal layer darker. Subsequently, however, the brightness in the basal layer gradually increased from day 4 (data not shown). This should be an effect produced by the newly synthesized melanin in the melanocytes. Melanocytes were visible in the RCM images probably because they accumulate melanosomes, which give strong contrast against the background (Fig 3*c* and *h*). Also, the following criteria support the view that the bright structures indicated by the arrows in Fig 3*h* correspond to melanocytes: (1) they are located in the epidermal basal layer, and elongate their dendrites to the upper spinous layer on the 3D imaging by RCM; (2) the brightness of the melanocytes shifted to surrounding keratinocytes in the RCM images taken thereafter.

Mizuno evaluated the changes in the melanocytes by examining skin biopsy specimens after a single UV exposure (2 MED). They reported that the DOPA reaction of the melanocyte became strong from day 4 after UV exposure. Furthermore, the dendrites of melanocytes that were poorly developed before UV exposure, elongated and thickened on days 6–8 after, and the melanocytes turned out to contain large DOPA-positive granules. Thus, it may take about 4 d for a large amount of melanin to be produced by the melanocytes after UV exposure. By the present RCM

methodology, we could observe for the first time the melanocytes non-invasively around 4 d after UV exposure and showed that their brightness increased gradually thereafter. These findings agreed roughly with those of Mizuno obtained by biopsy. These results indicate that RCM can be used to examine the activity of melanocytes by assessing melanin in the epidermal basal layer.

Our study evidenced RCM as a useful tool to address non-invasively the melanin distribution and synthesis in the skin *in vivo*.

Materials and Methods

Human subjects and animals This study was conducted according to Declaration of Helsinki Principles and approved by the ethics committee for human studies of our company. Healthy Japanese volunteers, who gave their informed consent, with Fitzpatrick's skin phototype III (Fitzpatrick, 1988) were enrolled. The skin of the volar and dorsal forearm was examined. Confocal microscopy imaging of the epidermal basal layer was performed at a constant light fluence. Additionally, an age-dependent pigmentary lesion located on the cheek of the volunteers was also imaged with careful monitoring of light power.

(HR-1 $\times$ HR/De) F_1 mice, an animal model for solar lentigo (Naganuma *et al*, 2001; Furuya *et al*, 2002) and Weiser–Maples strain guinea-pigs were developed at the Shiseido Research Center (Yokohama, Japan), and selected for this study. Furthermore, the skin of a Yucatan micropig was purchased from Charles Rivers Laboratories (Wilmington, Massachusetts), and examined as described below.

RCM imaging A commercially available RCM (Vivascope1000, Lucid, Henrietta, New York), which has been described previously (Rajadhyaksha *et al*, 1995, 1999), was used. The microscope uses an 830 nm diode laser operating at a power less than 20 mW. The power and the detection gain were maintained constant throughout the measurements before and after the UV exposure experiments (see Fig 3). For the objective lens, a $\times$ 50 oil immersion lens (Nikon, Tokyo, Japan) of numerical aperture 0.85 NA was selected. This lens was selected because during RCM imaging, a high reflection occurs because of the interface between stratum corneum and the mounting medium for the objective lens. The use of oil as the mounting medium avoided the high reflection and the oil immersion system was effective for the observation of thinner epidermis, for instance, mice skin. In our study, the field of view area of the confocal images was 450 $\times$ 350 μm. This RCM enables one to observe the specific horizontal reflectance image at a specific depth in the skin. For adjustment of the observation position, we controlled the Z-axis (vertical) with an electric stepping motor, and the X–Y axis (horizontal) manually using a micrometer.

Histology

DOPA staining For visualization of melanocytes existing in pigmented spots of (HR-1 $\times$ HR/De) F_1 mice, we prepared epidermal sheets of the back skin that were separated by immersing in aqueous 2 M NaBr solution, previous to the staining reaction with DOPA (Quevedo *et al*, 1969).

Fontana–Masson staining Skin samples obtained from the back of a Yucatan micropig and Weiser–Maples guinea-pig were fixed in 10% buffered formalin (pH 7.4). After embedding in paraffin, tissue sections (5 μm) were processed and stained with the Fontana–Masson method for the visualization of melanin distribution in epidermis.

Irradiation protocol for human skin A solar simulator from Electro Powerpacs (Solar Light, Philadelphia, Pennsylvania), equipped with xenon lamps as light source was used for irradiating UV, at a fluence rate of 0.385 mW per cm^2 at 297 nm. The MED of UV was determined by exposing seven spots on the volar forearm skin of three subjects with increments of 1.2. The MED was evaluated visually 24 h after UV exposure. Then, the dose of 2.5 MED was selected for examining the skin reaction after a single UV exposure, mainly by RCM imaging for a period of 70 d. Melanin and erythema indexes, automatically obtained with a Mexameter MX-16^{TM} (Courage + KHAZAKA Electronic GmbH, Köln, Germany), were also followed. A video microscope, HK-2200MD3 (Hirox, Tokyo, Japan) equipped with a $\times$ 20 magnification lens, was used for photographing the skin surface.

We are grateful to Mr Ritsuro Ideta and Mrs Rikako Furuya from Shiseido Research Center for providing (HR-1 $\times$ HR/De) F_1 mice.

Supplementary Material

The following material is available from http://www.blackwellpublishing.com/products/journals/suppmat/JID/JID23562/JID23562sm.htm

Figure S1

Time course of melanin and erythema changes after UV exposure. Photographs of the human volar forearm skin (skin type III) were taken along the time after a single UV exposure (2.5 MED), as indicated in the upper panels. The melanin and erythema indexes were evaluated by a Mexameter MX-16^{TM}, and shown in (*a*) and (*b*), respectively. The mexameter is equipped with LED (light emitting diode) light sources and a silicon diode detector for detecting reflected light from the skin. The instrument measures the intensity of reflected green (I_{green}: 568 nm), red (I_{red}: 660 nm) and infrared ($I_{infrared}$: 880 nm). The definitions of the melanin and erythema indexes calculated automatically by the Mexameter are as follows:

$$\text{Melanin index} : M = 500/\log 5\,(\log I_{infrared} - \log I_{red}) + 500$$

$$\text{Erythema index} : E = 500/\log 5\,(\log I_{red} - \log I_{green}) + 500$$

The results showed that the erythema was severest on day 2. The maximum darkening was observed on day 8. The melanin index did not return to the original state even on day 70, which was supported by RCM imaging.

DOI: 10.1111/j.0022-202X.2004.23562.x

Manuscript received April 9, 2004; revised September 10, 2004; accepted for publication September 20, 2004

Address correspondence to: Toyonobu Yamashita, Shiseido Research Center, 2-2-1 Hayabuchi, Tsuzuki-ku, Yokohama 224-8558, Japan. Email: toyonobu.yamashita@to.shiseido.co.jp

References

Byers HR, Maheshwary S, Amodeo DM, Dykstra SG: Role of cytoplasmic dynein in perinuclear aggregation of phagocytosed melanosomes and supranuclear melanin caps formation in human keratinocytes. J Invest Dermatol 121:813–820, 2003

Corcuff P, Betrand C, Leveque JL: Morphometry of human epidermis *in vivo* by real-time confocal microscopy. Arch Dermatol Res 285:475–481, 1993

Fitzpatrick TB: The validity and practicality of sun reactive skin types I though VI. Arch Dermatol 124:869–871, 1988

Furuya R, Akiu S, Ideta R, Naganuma M, Fukuda M, Hirobe T: Changes in the proliferative activity in epidermal melanocytes in serum-free primary culture during the development of ultraviolet radiation B-induced pigmented spots in hairless mice. Pigment Cell Res 1:348–356, 2002

Gates RR, Zimmermann AA: Comparison of skin color with melanin content. J Invest Dermatol 21:339–348, 1953

Hara M, Yaar M, Byers HR, Goukassian D, Fine RE, Gonsalves J, Gilchrest BA: Kinesin participates in melanosomal movement along melanocyte dendrites. J Invest Dermatol 114:438–443, 2000

Huzaira M, Rius F, Rajadhyaksha M, Anderson RR, González S: Topographic variations in normal skin, as viewed by *in vivo* reflectance confocal microscopy. J Invest Dermatol 116:846–852, 2001

Jimbow K, Quevedo WC Jr, Fitzpatrick TB, Szabo G: Some aspects of melanin biology: 1950–75. J Invest Dermatol 67:72–89, 1976

Jimbow K, Uesugi H: New melanogenesis and photobiological processes in activation and proliferation of precursor melanocytes after UV-exposure: Ultrastructural differentiation of precursor melanocytes from langerhans cells. J Invest Dermatol 78:108–115, 1982

Klaus SN: Pigment transfer in mammalian epidermis. Arch Dermatol 100: 756–762, 1969

Kobayashi N, Nakagawa A, Muramatsu T, *et al*: Supranuclear melanin caps reduce ultraviolet induced DNA photoproducts in human epidermis. J Invest Dermatol 110:806–810, 1998

Marks MBS, Seabra M: The melanosome: Membrane dynamics in black and white. Nat Rev 2:738–748, 2001

Minwalla L, Zhao Y, Poole CL, Wickett RR, Boissy RE: Keratinocytes play a role in regulating distribution patterns of recipient melanosomes *in vitro*. J Invest Dermatol 117:341–347, 2001

Mizuno N: Behavior of melanocyte after single ultraviolet radiation. Rinsyo Hifu 22:131–143, 1968

Montagna W, Carlisle K: The architecture of black and white facial skin. J Am Acad Dermatol 24:929–937, 1991

Mottaz JH, Zelickson AS: Melanin transfer: A possible phagocytic process. J Invest Dermatol 49:605–610, 1967

Naganuma M, Yagi E, Hara E, Fukuda M: Delayed induction of pigmented spots on UVB-irradiated hairless mice. J Dermatol Sci 25:29–35, 2001

Quevedo WC, Szabo G, Virks J: Influence of age and UV on the populations of DOPA-positive melanocytes in human skin. J Invest Dermatol 52: 287–290, 1969

Rajadhyaksha M, González S, Zavislan JM, Anderson RR, Webb RH: *In vivo* confocal scanning laser microscopy of human skin II: Advances in instrumentation and comparison with histology. J Invest Dermatol 113: 293–303, 1999

Rajadhyaksha M, Grossman M, Esterowitz D, Webb RH, Anderson RR: *In vivo* confocal scanning laser microscopy of human skin: Melanin provides strong contrast. J Invest Dermatol 104:946–952, 1995

Swindle LD, Thomas SG, Freeman M, Delaney PM: View of normal human skin *in vivo* as observed using fluorescent fiber-optic confocal microscopic imaging. J Invest Dermatol 121:706–712, 2003

Szabo G: Racial differences in the fate of melanosome in human epidermis. Nature 222:1081, 1969